The phospholipase A_2 enzyme complex PAFAH Ib mediates endosomal membrane tubule formation and trafficking

Marie E. Bechler, Anne M. Doody*, Kevin D. Ha, Bret L. Judson†, Ina Chen, and William J. Brown
Department of Molecular Biology and Genetics, Cornell University, Ithaca, NY 14853

ABSTRACT **Previous studies have shown that membrane tubule–mediated export from endosomal compartments requires a cytoplasmic phospholipase A_2 (PLA_2) activity. Here we report that the cytoplasmic PLA_2 enzyme complex platelet-activating factor acetylhydrolase (PAFAH) Ib, which consists of α1, α2, and LIS1 subunits, regulates the distribution and function of endosomes. The catalytic subunits α1 and α2 are located on early-sorting endosomes and the central endocytic recycling compartment (ERC) and their overexpression, but not overexpression of their catalytically inactive counterparts, induced endosome membrane tubules. In addition, overexpression α1 and α2 altered normal endocytic trafficking; transferrin was recycled back to the plasma membrane directly from peripheral early-sorting endosomes instead of making an intermediate stop in the ERC. Consistent with these results, small interfering RNA–mediated knockdown of α1 and α2 significantly inhibited the formation of endosome membrane tubules and delayed the recycling of transferrin. In addition, the results agree with previous reports that PAFAH Ib α1 and α2 expression levels affect the distribution of endosomes within the cell through interactions with the dynein regulator LIS1. These studies show that PAFAH Ib regulates endocytic membrane trafficking through novel mechanisms involving both PLA_2 activity and LIS1-dependent dynein function.**

Monitoring Editor
Vivek Malhotra
Centre for Genomic Regulation

Received: Dec 22, 2009
Revised: May 2, 2011
Accepted: May 6, 2011

INTRODUCTION

Trafficking through the endocytic pathway involves an ordered set of transport steps that moves both membrane-bound and soluble cargo between different compartments (Bonifacino and Glick, 2004; Maxfield and McGraw, 2004). Most endocytic compartments in mammalian cells, especially early-sorting endosomes and the endocytic recycling compartment (ERC), are morphologically complex tubulovesicular structures consisting of a mosaic of phosphoinositides, regulatory proteins, and other effectors (Marsh *et al.*, 1986; Miaczynska and Zerial, 2002; Maxfield and McGraw, 2004; He *et al.*, 2008). Sorting and export out of endocytic compartments has long been recognized to involve membrane tubules that emanate from the main vacuolar domain (Geuze *et al.*, 1983b). On the basis of geometry alone, thin membrane tubules (60–80 nm in diameter) serve as efficient sorting structures to separate membrane lipids and proteins from soluble internal contents (Rome, 1985). Early studies showed that many itinerant receptors become concentrated into tubular domains of endosomes for efficient export (Geuze *et al.*, 1983a, 1987; Stoorvogel *et al.*, 1987). These tubular extensions may function as platforms for the budding of coated vesicles or may detach to serve as trafficking intermediates (Bonifacino and Rojas, 2006).

The molecular mechanisms that mediate the formation of endosome membrane tubules are unclear. Rabs and other molecules have been shown to be involved in the formation of tubular domains on endosomes and to function in export from these organelles. For example, sorting nexins (Cullen, 2008) and Rab7 (Rojas *et al.*, 2008) facilitate the tubule-mediated sorting of itinerant endocytic cargoes. In addition, pharmacological and biochemical studies have suggested that phospholipid remodeling by cytoplasmic phospholipase A_2 (PLA_2) enzymes plays an important role in the

This article was published online ahead of print in MBoC in Press (http://www.molbiolcell.org/cgi/doi/10.1091/mbc.E09-12-1064) on May 18, 2011.

Present addresses: *Department of Biomedical Engineering, Cornell University, Ithaca, NY 14853; †Weill Institute for Cell and Molecular Biology, Cornell University, Ithaca, NY 14853.

Address correspondence to: William J. Brown (wjb5@cornell.edu).

Abbreviations used: BFA, brefeldin A; ERC, endocytic recycling compartment; LIS1, lissencephaly 1; PAFAH Ib, platelet activating factor acetylhydrolase Ib; PIPs, phosphoinositide phosphates; PLA2, phospholipase A2; TfR, transferrin receptor.

formation of endosome membrane tubules (Brown *et al.*, 2003). For example, a broad spectrum of PLA_2 antagonists inhibit the formation of endosome membrane tubules in vivo and in a cytosol-dependent in vitro reconstitution system (de Figueiredo *et al.*, 2001). In addition, these PLA_2 antagonists inhibit the export of transferrin (Tf) and Tf receptors (TfR) from early-sorting endosomes and the ERC. These results strongly suggest that a cytoplasmic PLA_2 functions in tubule-mediated export at each of these endosomal compartments.

The identity of cytoplasmic PLA_2 enzymes involved in the formation of endosomal membrane tubules has remained elusive. Here we show that the catalytic subunits of platelet-activating factor acetylhydrolase (PAFAH) Ib are endosome-associated PLA_2 enzymes that mediate tubule formation and route endocytic receptors for recycling. PAFAH Ib was originally purified based on its ability to hydrolyze an acetyl group in the *sn-2* position of the signal transduction phospholipid platelet-activating factor (PAF) (Hattori *et al.*, 1993). It is a multi-subunit complex consisting of a dimer of two highly conserved catalytic subunits, α1 (*Pafah1b3*) and α2 (*Pafah1b2*), and an associated noncatalytic subunit, β (*Pafah1b1*) (Arai, 2002). Within a species, α1 and α2 subunits share ~60% amino acid identity and by themselves can form catalytically active homodimers or heterodimers (Manya *et al.*, 1999). The β subunit, also known as LIS1, is highly conserved from yeast to humans, and mutations in it lead to the fatal brain disorder Miller–Dieker lissencephaly (Kato and Dobyns, 2003). Independent of binding to α1 or α2, LIS1 regulates the location of dynein on microtubules through the combined activities of a host of accessory proteins, including NudE and NudEL (Yamada *et al.*, 2008; Lam *et al.*, 2010). LIS1, NudE, and NudEL are responsible for nuclear trafficking in yeasts, spindle orientation, and neuronal migration in mammals, the last being compromised in human lissencephaly (Vallee and Tsai, 2006; Kerjan and Gleeson, 2007).

Although PAFAH Ib has been implicated in a wide array of processes, its exact biological function is unclear. Mice with targeted disruption of both *Pafah1b2* and *Pafah1b3* genes ($\alpha1^{-/-}$/$\alpha2^{-/-}$) exhibit defects in spermatogenesis but are otherwise normal (Koizumi *et al.*, 2003; Yan *et al.*, 2003). In contrast, recent studies using overexpression and small interfering RNA (siRNA)–mediated knockdown of α1 and α2 in cultured cells showed that PAFAH Ib α1 and α2 function to mediate the functional organization of the Golgi complex and secretion (San Pietro *et al.*, 2009; Bechler *et al.*, 2010). These results show that PAFAH Ib has an unexpected role in intracellular membrane trafficking. Here we show that this role is not limited to secretion. We found that α1 and α2 are partially localized to endosomes and that overexpression of either subunit induces endosome membrane tubule formation and alters the recycling route of endocytosed Tf and TfRs. Conversely, siRNA-mediated knockdown of α1 or α2 in cultured cells inhibited endosome tubule formation and delayed the recycling of Tf. These results demonstrate a novel mechanism for mediating endosome membrane trafficking and a new physiological role for PAFAH Ib enzymes.

RESULTS

PAFAH Ib α1 and α2 are found on early-sorting endosomes and the endocytic recycling compartment

The intracellular location of PAFAH Ib α1 and α2 has not been well documented. One study found green fluorescent protein (GFP)–tagged α1 diffuse in the cytoplasm, in the nucleus, and on juxtanuclear structures that resemble the Golgi complex (Smith *et al.*, 2000). We confirmed this localization pattern in cells transfected with hemagglutinin (HA)-tagged α1 and α2 (Bechler *et al.*, 2010). In addition, we found that α1-HA and α2-HA were located on peripheral cytoplasmic puncta that colocalized with the early endosome proteins EEA1 and GFP-Rab5 (Figure 1, A and B; Supplemental Figure S1A). At higher magnifications, the mosaic nature of this compartment was revealed, as EEA1 was confined to the spherical domain, whereas α1-HA could also be found on tubular extensions (Supplemental Figure S1A). PAFAH Ib α1 and α2 have conserved lipase motifs, and changing the serine residues in these motifs (α1 S47A; α2 S48A) renders the subunits catalytically inactive (Hattori *et al.*, 1994). We found that α1 S47A and α2 S48A were still partially localized to EEA1-positive early-sorting endosomes in transfected cells, demonstrating that catalytic activity is not required for organelle targeting (Supplemental Figure S1B; unpublished data). In addition to peripheral early-sorting endosomes, HA-tagged α1 and α2 were found on the centrally located ERC, as determined by colocalization with the ERC marker GFP-Rab11 (Figure 1, C and D). Localization of α1 or α2 on late endosomes/lysosomes was not observed (Supplemental Figure S1C).

To obtain complementary evidence that α1 and α2 subunits bind to endosome and Golgi membranes, we investigated the potential molecular mechanisms responsible for these interactions. It is well established that phosphoinositol phosphates (PIPs) serve as organelle landmarks and platforms for many cytoplasmic proteins that regulate membrane trafficking (Sato *et al.*, 2001). The cytoplasmic surface of Golgi membranes is enriched in PI(4)P and endosomes in PI(3)P, which mediate the binding of specific effector proteins. Using dot blot (PIP strip) overlays, we found that α1 binds specifically to PI(3)P and PI(4)P, and α2 to PI(3)P (Figure 1E). These results are consistent with the in vivo localization studies and suggest a mechanism by which α1 and α2 are recruited to endosome and Golgi membranes.

Overexpression of α1 or α2 alters the location of endocytic compartments

Whereas α1 and α2 were found on early-sorting endosomes and recycling endosomes, we observed that the distribution of early and late endosomes, but not that of recycling endosomes, was altered by overexpression (Figure 2). Both early and late endosomes appeared to be dispersed to the periphery, similar to defects in dynein-dependent endosome transport to the centrosome (Burkhardt *et al.*, 1997; Harada *et al.*, 1998; Valetti *et al.*, 1999; Liang *et al.*, 2004). The overexpression of α1 or α2 has been shown to affect LIS1–dynein interactions by sequestering LIS1 away from dynein (Yamaguchi *et al.*, 2007), resulting in dispersed membrane organelles (Ding *et al.*, 2009).

To test whether this redistribution is dependent on α1 and α2 catalytic activity, LIS1 binding, or both, we expressed the catalytic mutant α1 S47A, the LIS1-binding mutant α1 E38D (Yamaguchi *et al.*, 2007), or the double mutant α1 S47A/E38D. The relative expression levels of overexpressed α1 and mutants were comparable (Bechler *et al.*, 2010). The overexpression of both catalytically active and inactive α1 S47A resulted in a peripheral distribution of late and early endosomes, whereas expression of the LIS1-binding mutant, α1 E38D, had normal endosome distribution, consistent with previous reports (Ding *et al.*, 2009). Likewise, the LIS1-binding-defective and catalytically inactive α1 S47A/E38D showed normal distribution of early and late endosomes (Figure 2). The endocytic recycling compartment, as seen by GFP-Rab11, appeared unaffected by the expression of α1 or the various α1 mutants.

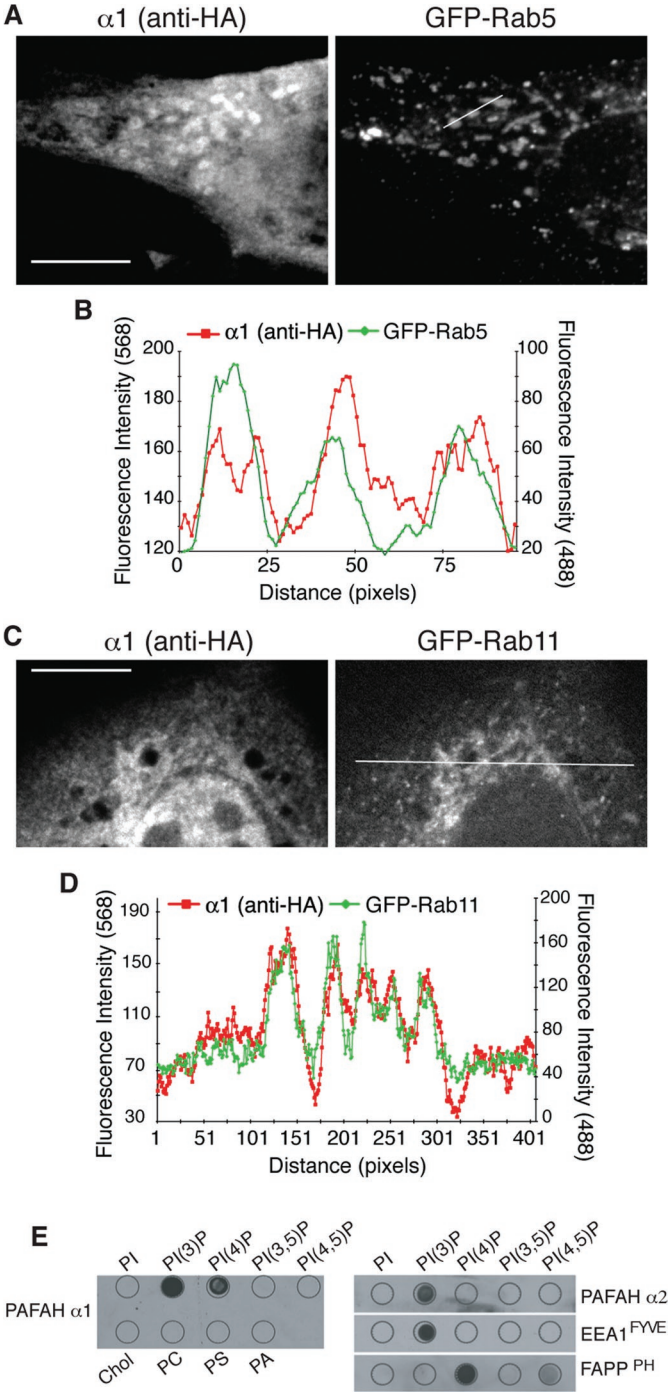

FIGURE 1: Localization of α1 to early and recycling endosomes. (A) HA-tagged α1 (anti-HA) was expressed and partially colocalized with the early-sorting endosome protein GFP-Rab5 in BTRD cells. (B) Line fluorescence intensity plot of α1 and GFP-Rab5 from A; line shown in the GFP-Rab5 image. (C) Cells expressing both α1-HA and GFP-Rab11 show that α1 colocalizes to the ERC. (D) Line fluorescence intensity plot of α1 and GFP-Rab11, from the line shown in the GFP-Rab11 confocal slice of C. Scale bars, 10 μm. Images shown are representative of more than five independent experiments. (E) Purified α1 and α2 specifically bind to PI(3)P and PI(4)P, and PI(3)P, respectively, on protein–lipid overlays. Purified EEA1^{FYVE} and FAPP^{PH} served as positive controls for PI(3)P and PI(4)P binding, respectively. Chol, cholesterol; PA, phosphatidic acid; PC, phosphatidylcholine; PI, phosphatidylinositol; PS, phosphatidylserine.

siRNA-mediated knockdown of α1 and α2 alters the localization of endocytosed transferrin and delays transferrin recycling

To investigate the potential role of PAFAH Ib PLA_2 subunits α1 and α2 in endocytic recycling, siRNA-mediated knockdown was conducted with siRNAs targeting both α1 and α2. A large assortment of cell lines was found to express both α1 and α2, and therefore it was necessary to transfect cells with an siRNA mixture to knock down both proteins. In BTRD cells, the mixed siRNAs reproducibly generated >80% reduction in α1 and α2 levels (Figure 3A).

Tf trafficking in cells with reduced α1 and α2 was monitored over a pulse-chase time course with fluorescein isothiocyanate (FITC)-Tf. Within 5 min of endocytosis, the amount of FITC-Tf was equivalent between α1 and α2 knockdown and control cells (Figure 3, B and C), indicating that knockdown did not affect endocytosis. Within 15 min of FITC-Tf endocytosis, there was an apparent difference between knockdown and control cells. In knockdown cells, FITC-Tf was clustered in a tight, central ERC-like location, with very few peripherally labeled endosomes (Figure 3, B and E). This became more evident by 45 min pulse. This distribution of FITC-Tf was also evident during chase of FITC-Tf out of the cells (Figure 3, B and E). In addition, during chase time points, α1 and α2 knockdown cells appeared to retain total FITC-Tf fluorescence over a longer period of time, indicating that the recycling of FITC-Tf was slowed (Figure 3, B and D).

Knockdown of α1 and α2 alters the distribution of early and late endosomes but not the endocytic recycling compartment

Because the distribution of FITC-Tf was affected by α1 and α2 knockdown, and overexpression affects the distribution of endosomes, we wanted to address whether the physical location of endosomes was affected with the reduction of α1 and α2. Therefore we analyzed the distribution of early endosomes, late endosomes, recycling endosomes, and lysosomes in α1 and α2 knockdown BTRD cells. Endosomes and lysosomes labeled with either EEA1, CD63, or cathepsin D, but not GFP-Rab11, were more clustered in the cell center with reduced α1 and α2 (Figure 4A). To determine whether this phenotype was due to decreased α1 and α2 PLA_2 activity or a consequence of reduced binding to LIS1, which regulates dynein activity (Tarricone *et al.*, 2004; Kardon and Vale, 2009), we expressed RNAi-resistant versions of α1 wild-type, catalytic inactive (α1 S47A), and binding mutants α1 E38D or α1 S47A/E38D in cells that were treated with α1 and α2 siRNAs. Cells expressing RNAi-resistant α1 or α1 S47A rescued the distribution of early and late endosomes, as well as lysosomes. In contrast, cells expressing LIS1-binding mutant versions displayed similar phenotypes to α1 and α2 knockdown cells (Figure 4, B–D), suggesting that endosome clustering is a result of lost α1 and α2 interactions with LIS1.

This redistribution of endocytic markers could result from physical relocation of endosomes, mistargeting of endocytic proteins, or enhanced fusion of early endosomes with late endosomes. To determine whether the endosome markers still appropriately localize to distinct early and late endosome organelles in α1 and α2 knockdown cells, double and triple labeling with Rab proteins was conducted. The reduction of α1 and α2 levels did not affect the colocalization of EEA1 with GFP-Rab4 or GFP-Rab5 (Supplemental Figure S2). Conversely, EEA1 did not localize to GFP-Rab7– or CD63-positive late endosomes (Supplemental Figure S2A; unpublished data). In addition, CD63 did not colocalize with GFP-Rab4 (Supplemental Figure S2A) but did colocalize appropriately with GFP-Rab7 (unpublished data).

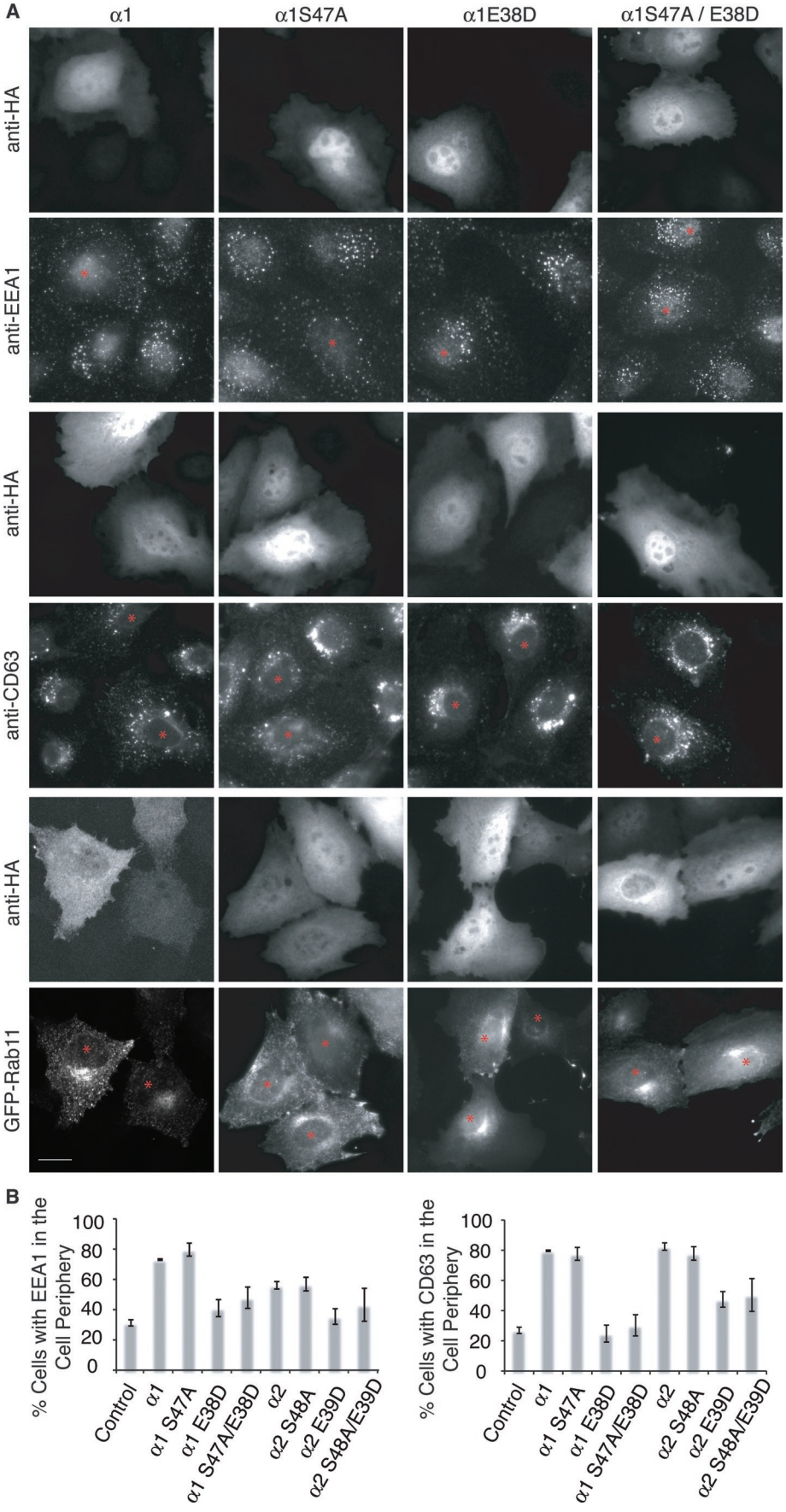

FIGURE 2: Overexpression of α1 or α2 redistributes early and late endosomes to the cell periphery. (A) Wide-field images of untransfected BTRD cells side by side with cells expressing either wild-type α1, catalytic inactive α1 S47A, LIS1-binding mutant α1 E38D, or double mutant α1 S47A/E38D (HA tagged) and colabeled with early (EEA1), late (CD63), or recycling endosome (GFP-Rab11) markers. Asterisk indicates transfected cells. (B) Quantification of the percentage of cells with endosomes, early (EEA1) or late (CD63), dispersed toward the cell periphery. Scale bar, 10 μm.

As a second test of endosome identity, we examined whether Tf is delivered to EEA1-labeled endosomes shortly after endocytosis. Within 5 min of internalization from the plasma membrane, proteins arrive in EEA1-labeled early endosomes but are not yet sorted to the ERC or late endosomes (Maxfield and McGraw, 2004). In both control and α1 and α2 knockdown cells, FITC-Tf internalized for 5 min colocalized with a subset of EEA1-labeled puncta, although FITC-Tf and EEA1 puncta were located in the center of α1 and α2 knockdown cells (Supplemental Figure S2C), indicating that Tf did reach functionally defined early endosomes.

PAFAH Ib α1 and α2 regulate endosome tubule formation

Early-sorting endosomes and the ERC are complex tubulovesicular organelles. At steady state, the tubular elements are difficult to image and quantify because they are highly dynamic. However, the tubular domains of endosomes become greatly enhanced when treated with brefeldin A (BFA), an inhibitor of coated vesicle formation (Lippincott-Schwartz *et al.*, 1991; Wood *et al.*, 1991; Wood and Brown, 1992). BFA provides a useful tool for investigating the molecular mechanisms required to make tubules. For example, previous studies showed that PLA_2 antagonists inhibit BFA-stimulated endosome tubule formation (de Figueiredo *et al.*, 2001). Therefore we asked whether α1 and α2 are required for BFA-stimulated tubule formation by performing siRNA-mediated knockdown experiments. In control cells, early endosomes and the ERC labeled with FITC-Tf rapidly undergo extensive tubule formation after addition of BFA, whereas the endosomes in siRNA-treated cells displayed many fewer tubules (Figure 5, A–C). Quantification of these results revealed that the extent of membrane tubule formation was reduced in knockdown cells (Figure 5B).

To determine whether, conversely, overexpression of α1 or α2 increased endosome tubule formation, we measured the percentage of endosomes that had tubular morphology in transfected and nontransfected

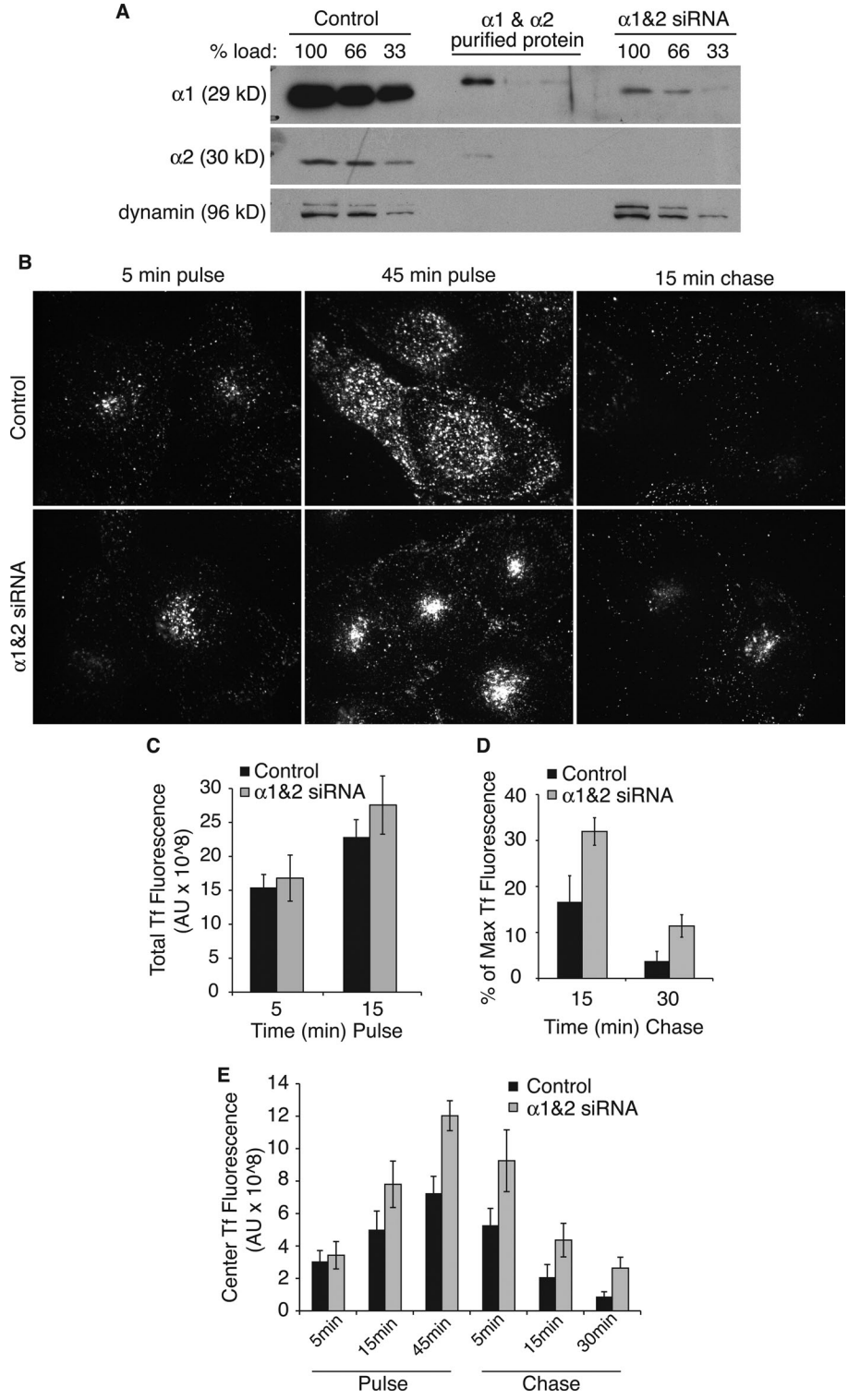

FIGURE 3: siRNA-mediated knockdown of α1 and α2 delays the recycling of transferrin. BTRD cells were transfected with control or α1 and α2 siRNAs 72 h before experimentation. (A) Western blots of BTRD cell lysates 72 h after siRNA transfection. (B) Pulse-chase experiments were conducted with FITC-Tf in control and α1 and α2 siRNA-treated cells. Cells were pulse labeled with FITC-Tf for 45 min, followed by chase in media containing unlabeled (nonfluorescent) Tf for 15 min. Representative confocal images are shown for the indicated time points. (C) Total FITC-Tf fluorescence was measured at 5 and 15 min after addition of FITC-Tf to the media (pulse). (D) At the indicated chase time points, Tf fluorescence remaining in cells was quantified and is shown as a percentage of the total Tf fluorescence after 45 min pulse (maximum Tf fluorescence). At 30 min, $p < 0.05$ by a *t* test. (E) The fluorescence intensity of the juxtanuclear, central FITC-Tf was measured at the indicated pulse and chase time points in control or α1 and α2 siRNA-treated cells. n = 4; error bars, SEM.

cells that had internalized TRITC-Tf or Alexa 488–Tf for 45 min, which labels both early and recycling endosome compartments. Overexpression of wild-type α1 or α2 caused endosomes to become more tubular. Long-axis lengths of sorting endosomes in control cells were 1.04 ± 0.2 μm versus 1.41 ± 0.3 μm in transfected cells (Figure 5D). In addition, the percentage of total endosomes with single or multiple tubules was significantly increased with overexpression of catalytically active α1 or α2 (Figure 5E). This tubule formation was dependent on catalytic activity because overexpression of catalytic mutants (α1 S47A or α2 S48A) did increase the fraction of tubulated endosomes. Because overexpression of α1 or α2 influenced the distribution of endosomes in an LIS1-dependent manner, we examined whether endosome tubule formation was similarly dependent. The results showed that overexpression of the catalytically active, LIS1-binding mutants (α1 E38D or α2 E39D) also increased endosome tubules, but the catalytically inactive, LIS1-binding double mutants did not (Figure 5E). These results demonstrate that PAFAH Ib increases endosome tubule formation by virtue of its phospholipase activity and not through altering LIS1-dependent effects on dynein function.

Overexpression of PAFAH Ib α1 or α2 alters trafficking through the endocytic recycling compartment

To investigate whether the overexpression of α1 and α2 may enhance endocytic trafficking, we examined the effect of overexpressing wild-type or mutant versions of α1 or α2 on trafficking of Alexa 488–labeled Tf (Tf-488). Only α1 is shown and discussed here, as results for α1 and α2 were comparable. Cells were incubated with media containing Tf-488 (pulse) for 45 min, followed by replacement of the media with unlabeled Tf (chase) for 40 min. The internalization of fluorescent Tf in 15 min was equivalent between control and all α1-overexpressing cells (Figure 6, A and B). Following a 45 min pulse of Tf-488 in untransfected cells or cells transfected with LIS1-binding mutants α1 E38D or α1 S47A/E38D, Tf-488 was localized to puncta throughout the cell, as well as clustered in the juxtanuclear ERC (Figure 6, A and C). However, in cells expressing wild-type α1 or α1 S47A, Tf localized only to puncta in the periphery. Similarly, TfRs were found peripherally distributed in α1 or α1 S47A-transfected HeLa cells, but TfR distribution was not affected in cells expressing LIS1-binding mutant constructs (Figure 6D).

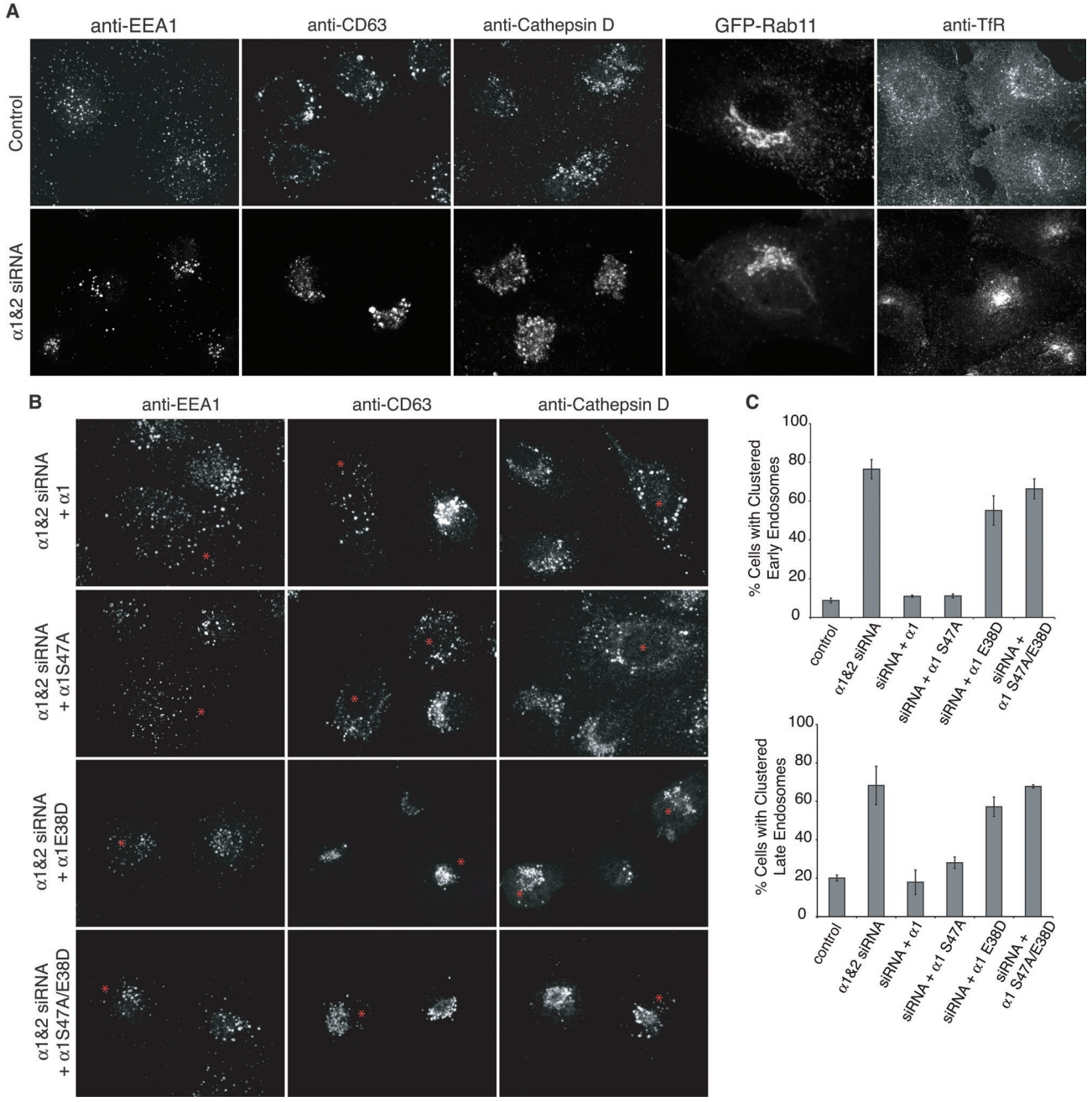

FIGURE 4: Endosome positioning is altered in α1 and α2 knockdown cells due to lost interactions with LIS1. (A) Confocal images of early endosomes (EEA1), late endosomes (CD63), lysosomes (cathepsin D), the transferrin receptor (TfR), or recycling endosomes visualized with expression of GFP-Rab11 in BTRD cells transfected with control RNA or siRNA targeting α1 and α2. (B) Confocal images of α1 and α2 siRNA-treated BTRD cells transfected with RNAi-resistant α1, catalytic inactive α1 S47A, LIS1-binding mutant α1 E38D, or double mutant α1 S47A/E38D. Wild-type α1 and catalytic inactive α1 S47A rescued endosome clustering seen with α1 and α2 knockdown, but LIS1-binding mutant (E38D) versions did not rescue changes in endosome distribution. Asterisk indicates cells transfected with α1 RNAi-resistant constructs, as determined by anti-HA staining. (C) Quantification of early and late endosome clustering in knockdown and RNAi-resistant α1 transfected cells as indicated. n = 3–4; error bars, SEM.

To compare Tf recycling, a chase with unlabeled Tf for 10, 20, or 40 min was conducted. In control cells and cells expressing LIS1-binding mutant versions of α1, Tf-488 accumulated in the central ERC; over the 40 min of chase, Tf-488 signal was progressively lost due to the recycling of Tf out of the cell and its release into the medium (Figure 6). The overexpression of α1 or α1 S47A did not have an effect on the kinetics of Tf recycling, but rather affected the route of Tf, as fluorescent Tf never accumulated in the ERC (Figure 6, A–C). These results suggest that overexpression of α1 or α2, likely by disrupting LIS1 activation of dynein (Yamaguchi *et al.*, 2007; Ding *et al.*, 2009; Lam *et al.*, 2010), reduced the transport of Tf from peripheral early-sorting endosomes to the central ERC, thus bypassing the ERC during the recycling to the cell surface. The overexpression of α1 E38D also did not interfere with the

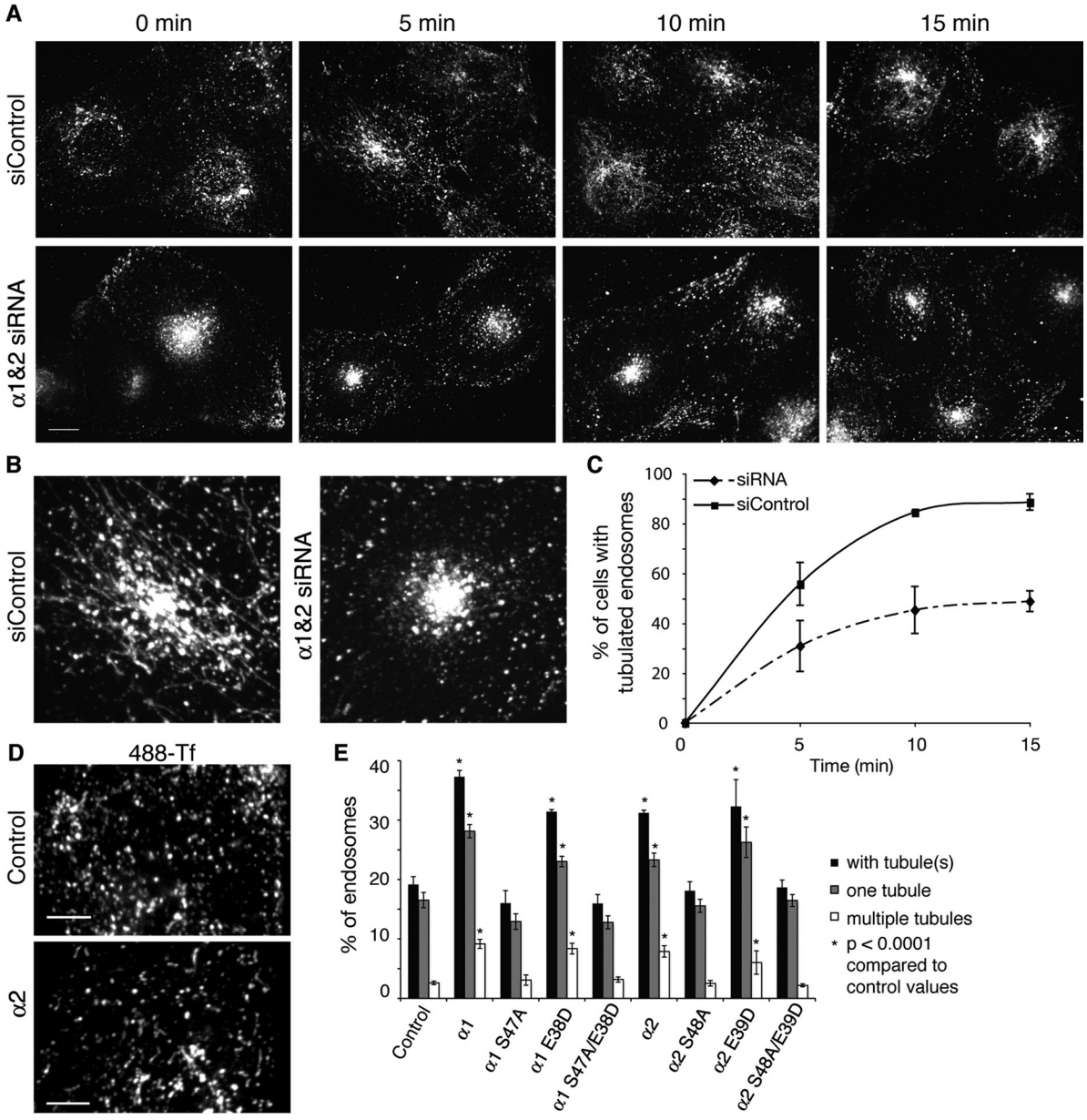

FIGURE 5: α1 and α2 knockdown inhibits BFA-stimulated tubulation of endosomes, and overexpression of α1 or α2 induces endosome tubule formation. (A) Cells transfected with control RNA or siRNAs against α1 and α2 were incubated with FITC-Tf for 45 min to label all early-sorting endosomes and the ERC, and then treated with BFA (5 μg/ml) in the continuous presence of FITC-Tf for the indicated times. Scale bar, 10 μm. (B) Magnified images of FITC-Tf–labeled endosomes in control and α1 and α2 siRNA-treated cells after 5 min of BFA treatment. (C) Quantification of BFA-stimulated tubulation in control and α1 and α2 siRNA-treated cells. n = 4; error bars, SEM. (D) Representative images of control HeLa cells and HeLa cells transfected with α2. Cells were incubated with Alexa 488–Tf for 45 min to label endocytic compartments. Scale bar, 5 μm. (E) Percentage of endosomes with membrane tubules in control cells or cells transfected with indicated versions of α1 or α2. More than 35 cells and 4500 endosomes were counted per condition, from a total of three independent experiments. Error bars = SEM. One-way ANOVAs were conducted to evaluate differences between conditions. The percentages of endosomes with membrane tubules for control, α1 S47A, α1 S47A/E38D, α2 S48A, and α2 S48A/E39D cells were not statistically different. The percentages of endosomes with membrane tubules for cells transfected with α1, α1 E38D, α2, or α2 E39D were all statistically different from control and catalytically inactive α1 and α2 counterparts with $p < 0.0001$ (asterisks).

recycling of Tf, since fluorescence of Tf-488 during chase time points was comparable to that of control cells (Figure 6B). There was, however, a noticeable lag in recycling kinetics with the double mutant α1 S47A/E38D. During chase time points, α1 S47A/E38D showed higher Tf-488 fluorescence in the cell, suggesting delayed recycling kinetics compared with α1 E38D and control cells.

DISCUSSION

These results reveal novel means for mediating endosome membrane trafficking and morphology with a new functional role for cytoplasmic PAFAH Ib α1 and α2. Overexpression of α1 or α2 had three clear phenotypic consequences: 1) redistribution of early and late endosomes toward the cell periphery; 2) recycling of Tf/TfR

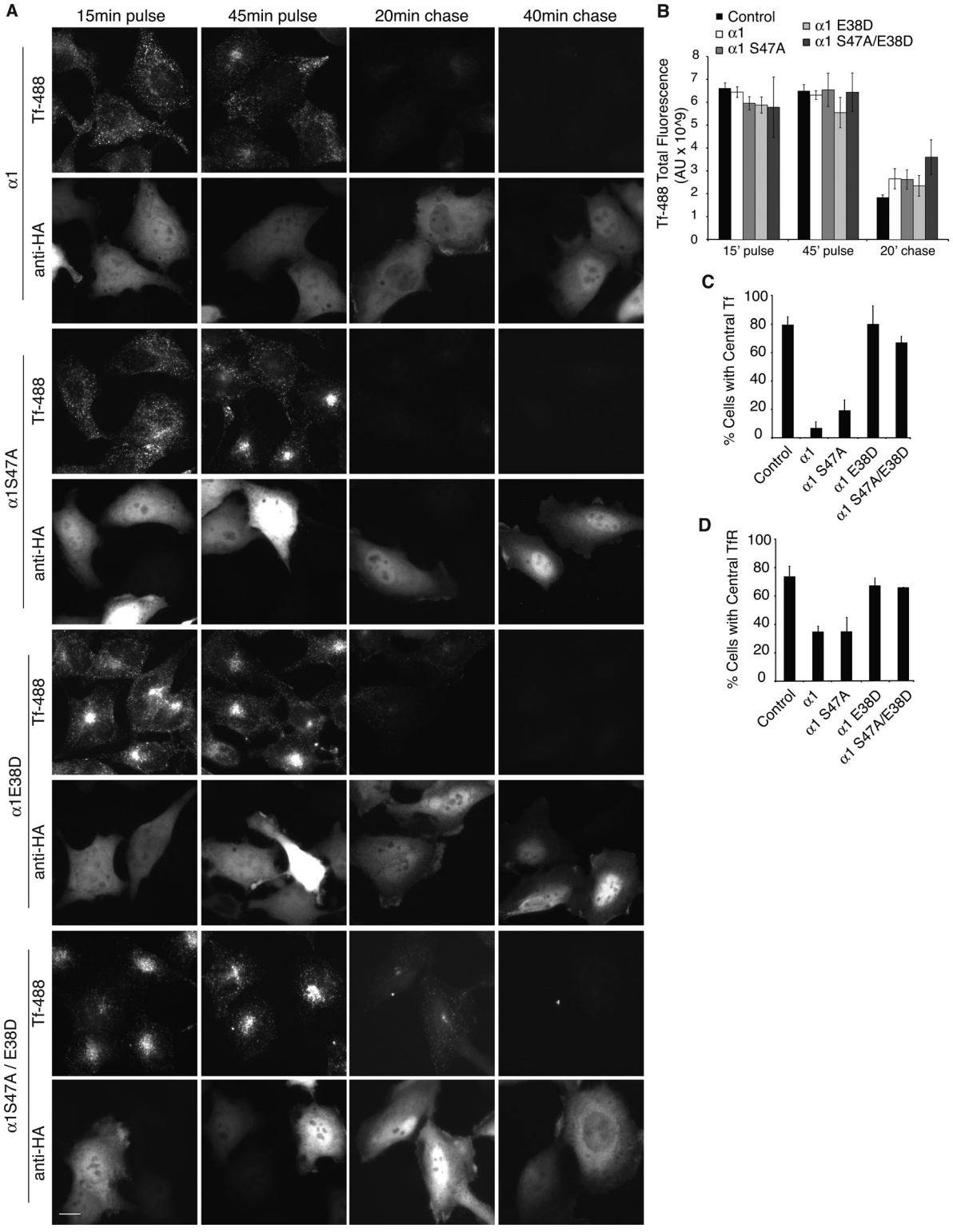

FIGURE 6: Overexpression of α1 reroutes Tf and the TfR traffic from early endosomes, bypassing the central endocytic recycling compartment, back to the plasma membrane, and double mutant α1 S47A/E38D slows Tf recycling. (A) HeLa cells were transiently transfected with α1-HA or α1 mutants and pulse labeled with Alexa 488–Tf (Tf-488) for 15 and 45 min, followed by chase in Tf-free media for 20 or 40 min to observe Tf internalization and recycling. Scale bar, 10 μm. (B) The fluorescence intensity of Alexa 488–Tf was measured for pulse and chase time points in untransfected (control) HeLa cells and cells expressing indicated proteins. α1 S47A/E38D compared with control or compared with α1 E38D is significantly different, with $p < 0.0001$ as analyzed by a *t* test. (C) Quantification of the percentage of cells with central (ERC) Tf fluorescence after a 45 min pulse of Alexa 488–Tf (Tf-488). (D) Percentage of cells with central Tf receptor (anti-TfR) fluorescence. Anti-TfR was used without colabeling with anti-HA, as the antibodies were both from mice. Therefore cell counts include both transfected and untransfected HeLa cells. Error bars, SEM.

from early-sorting endosomes to the plasma membrane, bypassing the ERC; and 3) stimulation of endosome tubule formation. These phenotypes were opposite to effects seen with loss of α1 and α2: 1) redistribution of early endosomes, late endosomes, and lysosomes to the cell center; 2) a delay in Tf recycling to the cell surface; and 3) inhibition of BFA-stimulated endosome tubules.

The altered organelle distribution observed by overexpression or knockdown of α1 and α2 could be explained by, respectively, increased or decreased interactions with LIS1. This would affect the fraction of LIS1 available to bind and activate dynein for minus end–directed microtubule transport (Tarricone *et al.*, 2004; Yamaguchi *et al.*, 2007). In effect, the overexpression or knockdown would decrease or increase, respectively, transport of endosomes and lysosomes toward the centrosome, which is a dynein-dependent function activated by LIS1 (Burkhardt *et al.*, 1997; Harada *et al.*, 1998; Liang *et al.*, 2004; Lam *et al.*, 2010). Our results are in agreement with reports that overexpression of α1 and α2 affect LIS1 binding and regulation of dynein in endosome and lysosome transport (Ding *et al.*, 2009).

The effects of α1 and α2 overexpression and knockdown on Tf recycling may be partially explained by interactions with LIS1. Pulse-chase experiments demonstrate that overexpression of wild-type and catalytically inactive α1 and α2 prevent transport of Tf from peripheral early-sorting endosomes to the ERC (Supplemental Figure S3, step C) but not the release of internalized Tf from the cell. These results strongly suggest that Tf is recycled directly from early-sorting endosomes rather than from the ERC (Supplemental Figure S3, step B). In fact, a portion of the endocytosed membrane and receptors are normally recycled from early-sorting endosomes directly back to the plasma membrane (Sheff *et al.*, 1999; Hao and Maxfield, 2000). This apparent rerouting of Tf and TfR did not occur with the overexpression of LIS1-binding-defective constructs, strongly suggesting that Tf and TfR may be shuttled directly from early endosomes to the plasma membrane due to decreased dynein activation by LIS1. This indicates that dynein activation by LIS1 is important for transport from early endosomes to the endocytic recycling compartment, a trafficking step that is dynein dependent and membrane tubule mediated (Maxfield and McGraw, 2004; Driskell *et al.*, 2007; Traer *et al.*, 2007). These results are reminiscent of dynein inactivation by the overexpression of dynamitin, which also shifts the route of Tf recycling directly from peripherally sorting endosomes but does not affect the kinetics of recycling (Valetti *et al.*, 1999). The binding of LIS1 by excess α1 or α2 (from overexpression) would decrease the activation of dynein-mediated transport of cargo, including Tf transport from the early-sorting endosomes to the ERC (Supplemental Figure S3C).

The catalytically inactive LIS1-binding mutant, α1 S47A/E38D, did not reroute Tf but did delay Tf recycling compared with control cells and α1 E38D-overexpressing cells. This catalytically inactive mutant (α1 S47A/E38D) may act as a dominant negative, which has been suggested by recent studies (Bechler *et al.*, 2010). Catalytically inactive subunits may dimerize with endogenous subunits, creating inactive, "poisoned" dimers. A dominant-negative effect by the catalytic mutant is consistent with knockdown experiments, which also showed a delay in Tf recycling. If catalytically inactive α1 (S47A) or α2 (S48A) acts as a dominant negative, one would predict that α1 S47A would also delay Tf recycling. A possible explanation to this apparent inconsistency is depicted in Supplemental Figure S3: α1 and α2 are important for membrane trafficking from early endosomes to recycling endosomes (step C) and/or from the ERC to the plasma membrane (step D) but not necessarily in the "short" recycling pathway directly from the early-sorting endosomes to the plasma membrane (step B). This is an appealing possibility that fits well with our observations. The overexpression of α1 or α2, each of which can bind LIS1, appears to dramatically inhibit dynein-dependent function, blocking early to recycling endosome transport (step C) and rerouting Tf to recycle from early endosomes to the plasma membrane (step B). Therefore no apparent dominant-negative phenotype would be seen, as the trafficking steps regulated by α1 and α2 would already be blocked by reduced dynein function. This suggests that α1 and α2 are important for transport from early endosomes to the ERC (step C) and/or from the ERC to the plasma membrane (step D).

We found that overexpression of α1 or α2 increased the number of tubulated peripheral endosomes, whereas α1 and α2 knockdown inhibited Tf-labeled endosome tubules. These changes in membrane tubule formation can be explained by the direct membrane-altering action of PAFAH Ib PLA_2 subunits, as catalytically inactive forms α1 S47A or α2 S48A did not increase endosome membrane tubules. The conclusion that α1 and α2 work directly on endosome membranes is supported by fluorescence imaging showing that both α1 and α2 are associated with Rab5- and EEA1-positive early-sorting endosomes and the Rab11-positive ERC. Consistent with these results, and with previous studies in which α1 and α2 were also localized to Golgi membranes, we found that α1 specifically interacted with endosome-enriched PI(3)P and Golgi-enriched PI(4)P, and α2 with PI(3)P. Of interest, neither α1 or α2 has any identifiable known PIP-binding motifs or domains, such as the FYVE domain of EEA1 that binds PI(3)P (Stenmark *et al.*, 1996; Burd and Emr, 1998). However, the crystal structure of PAFAH Ib reveals the presence of a small surface cluster of basic residues (Ho *et al.*, 1997), which could be functionally similar to the basic residue clusters used by PH and FYVE domains to bind phosphate groups of PIPs (Lemmon, 2008).

There is growing evidence that cytoplasmic PLA enzymes contribute to the formation of membrane tubules and regulate trafficking (de Figueiredo *et al.*, 1998, 1999, 2000; Polizotto *et al.*, 1999). The hydrolytic activity of α1 or α2 may contribute to the formation of membrane tubules by removal of *sn*-2–position acyl chains from phospholipids, resulting in a shift from cylindrical or cone-shaped phospholipids to inverted-cone–shaped lysophospholipids (Brown *et al.*, 2003). Localized accumulation of lysophospholipids creates tighter packing of the acyl chains in one leaflet of the membrane bilayer, resulting in outward curvature of the membrane that could then grow into a tubule (Sheetz and Singer, 1974; Zimmerberg and Kozlov, 2006). Alternatively, the lipid-modifying activity of α1 and α2 may feed into lipid-modifying pathways that can either directly affect membrane curvature or act indirectly by recruiting proteins that bend membranes.

In recent work, three phospholipases have been shown to be involved in Golgi structure and function. The cytoplasmic Ca^{2+}-dependent enzyme $cPLA_2\alpha$ was shown to be recruited to the Golgi following an increase in secretory load and to enhance intra-Golgi membrane tubules that facilitate anterograde transport through the Golgi stack (San Pietro *et al.*, 2009). $cPLA_2\alpha$ was also found to be required for export of junctional proteins in polarized endothelial cells (Regan-Klapisz *et al.*, 2009). PLA2G6-A was shown to be required for tubule-mediated assembly of the endoplasmic reticulum-Golgi intermediate compartment (Ben-Tekaya *et al.*, 2010). Finally, in other studies, we have found that PAFAH Ib α1 or α2 is also localized to the Golgi complex, where it mediates tubule formation and secretory trafficking (Bechler *et al.*, 2010). These results, along with studies described here, establish that α1 or α2 function at multiple organelles.

Our studies identify a specific cytoplasmic PLA_2, PAFAH Ib, that is capable of inducing membrane tubule formation and altering endocytic membrane trafficking pathways. Furthermore, these results demonstrate a physiological role for PAFAH Ib in mediating intracellular membrane trafficking. Although it is possible that some effects of PAFAH Ib on endosomes are indirectly caused by α1- and α2-mediated changes in Golgi function (the converse is possible as well), our experiments cannot resolve this issue. Future research should further address how PAFAH Ib selectively interacts with endosome and Golgi membranes and whether it interacts with other molecules, for example, Rabs, sorting nexins, and phosphoinositides, to facilitate efficient endosomal sorting. Nevertheless, this work and the recent work of others demonstrate the importance of lipid-modifying enzymes in both secretory and endocytic trafficking.

MATERIALS AND METHODS

Materials and reagents

Brefeldin A was obtained from BIOMOL Research Laboratories (Enzo Life Sciences, Plymouth Meeting, PA). Stock solutions of BFA (in ethanol) were stored at −20°C and diluted to working concentrations just before use. Tetramethylrhodamine-conjugated transferrin (TRITC-Tf), Alexa 488–conjugated human transferrin (Tf-488), and bovine holo transferrin were purchased from Invitrogen (Carlsbad, CA). Fluorescein isothiocyanate was from Sigma-Aldrich (St. Louis, MO).

We prepared guinea pig polyclonal anti-α1 antibodies, purchased chicken anti-α2 (Abcam, Cambridge, MA), and received rabbit polyclonal anti-dynamin antibodies from M. McNiven (Mayo Clinic, Rochester, MN) for Western blot analyses. Unfortunately, these antibodies have not been useful for immunofluorescence. Mouse monoclonal anti–human influenza virus hemagglutinin was purchased from Covance (Berkeley, CA). Rabbit polyclonal anti–early endosomal antigen 1 (EEA1) was purchased from ABR Affinity BioReagents (Golden, CO) and Cell Signaling Technology (Beverly, MA). Mouse anti–human transferrin receptor was obtained from Zymed (Invitrogen). Rabbit polyclonal antibodies against the late endosome/lysosome marker CD63 and lysosomal marker cathepsin D were prepared and characterized as described (Park *et al.*, 1991; Heller *et al.*, 1994). The secondary fluorescent antibodies goat anti-mouse or goat anti-rabbit conjugated to FITC, TRITC, Cy5, or DyLight were purchased from Jackson ImmunoResearch Laboratories (West Grove, PA). The anti-mouse conjugated to Alexa Fluor 488 was from Molecular Probes (Invitrogen). Horseradish peroxidase (HRP)–conjugated antibodies were as follows: goat anti-chicken (Aves Labs, Tigard, OR), anti–guinea pig (Pocono Rabbit Farm and Laboratory, Canadensis, PA), and anti-rabbit (GE Healthcare Biosciences, Piscataway, NJ). Human cDNA of Rab11 and Rab4 in pEGFP vectors, GFP-Rab11, and GFP-Rab4 were the kind gifts of M. Scidmore (Cornell University, Ithaca, NY). Human Rab5A cDNA in the pGreenLantern vector GFP-Rab5 was the gift of C. Roy (Yale University, New Haven, CT).

Preparation of plasmids for mammalian expression

PAFAH Ib α1-HA and α2-HA were constructed by inserting internal HA tags at G165 and P130, respectively. The HA tags were inserted by PCR, using pUC-P_L-cI-α1 and pUC-P_L-cI-α2 as templates. pEGFP-N1 from BD Biosciences Clontech (Mountain View, CA) was digested with *Eco*RI and *Xba*I to remove the GFP gene and generate pEN1. The PCR fragments encoding α1-HA and α2-HA were ligated into *Eco*RI/*Xba*I–digested pEN1 to generate pEN1-α1-HA and pEN1-α2-HA. pEN1-α2-S48A-HA was constructed by site-directed mutagenesis of a single nucleotide. RNAi-resistant pEN1-α1-HA and pEN1-α1-S47A-HA were generated by making two silent mutations in the double-stranded RNA target sequence. LIS1-binding mutants α1 E38D or α2 E39D (Yamaguchi *et al.*, 2007) were generated by site-directed mutagenesis of RNAi-resistant pEN1-α1-HA, pEN1-α2-HA, pEN1-α1-S47A-HA, and pEN1-α2-S48A-HA.

Cell culture, transfection, and immunocytochemistry

Human epithelial (HeLa) cells and transformed bovine testicular (BTRD) cells were grown in modified Eagle's minimal essential medium (MEM) with 10% Nu-Serum or 10% bovine growth serum from Life Technologies (Carlsbad, CA) or Thermo Scientific HyClone (Logan, UT). All cells were maintained at 37°C in a humidified atmosphere of 95% air, 5% CO_2.

HeLa and BTRD cells were transfected using Lipofectamine 2000 (Invitrogen). Cells were grown on glass coverslips for 1–2 d before experimentation. Lipofectamine 2000 was used as described in the manufacturer's protocol with modifications: one-fourth of the listed DNA and transfection reagent were used, as higher quantities resulted in cell death. Transfection efficiencies of 50–80% were possible with this alteration. Cells were used for experimentation 24–48 h after addition of the transfection mix.

For RNAi, cells were transfected on two consecutive days with Lipofectamine RNAiMax (Invitrogen) and 30 nM of double-stranded RNAs. RNAs were designed through Thermo Scientific (Dharmacon) custom siRNA oligo service to target bovine α1 mRNA and bovine α2 mRNA. The sense oligonucleotide sequences are AGAAUGGAGAGCUGGAACAUU and GGAGAACUGGAGAAUAUUAUU for α1 and α2, respectively. Control duplex RNA (siControl) sequences were verified by the Basic Local Alignment Search Tool to have no significant identity to any other sequence in the bovine genome: siGenome nontargeting siRNA #1 and #2. Cells were used for experiments 72 h after the initial RNA transfection.

Cells were processed for indirect immunofluorescence as described (de Figueiredo *et al.*, 2001). Primary antibodies were used at the following dilutions: monoclonal anti-HA at 1:100; polyclonal anti-EEA1 at 1:100; monoclonal anti-TfR at 1:200; polyclonal anti-CD63 at 1:200; polyclonal rabbit anti–cathepsin D at 1:200. Secondary antibodies were used at the following dilutions: FITC-, TRITC-, or Cy5-labeled anti–mouse immunoglobulin G (IgG) or anti–rabbit IgG at 1:100; Alexa 488–labeled anti–mouse IgG at 1:500; and DyLight anti-rabbit at 1:100. Coverslips were mounted with Vectashield mounting media (Vector Laboratories, Burlingame, CA) and stored at −20°C until imaged.

Cell lysates and immunoblotting

Cells were lysed by scraping dishes in the presence of 0.05% Triton X-100 in phosphate-buffered saline, pH 7.4, and complete protease inhibitor cocktail (Roche Applied Science, Mannheim, Germany). Lysates and purified proteins were run by SDS–PAGE, transferred to PVDF membranes, and Western blotted with the antibodies guinea pig anti-α1 (1:2000) and chicken anti-α2 (1:1000), and rabbit anti-dynamin (1:10,000) was used as an internal loading control. HRP-conjugated antibodies were goat anti-guinea pig (1:2500), goat anti-chicken (1:2500), and goat anti-rabbit (1:10,000). HRP was detected with Millipore (Billerica, MA) enhanced chemiluminescent reagent. Band intensities were quantified using ImageJ software (National Institutes of Health, Bethesda, MD), and background intensity was subtracted and normalized to the corresponding anti-dynamin band for each lane.

Lipid-protein overlays

Stock lipids (Avanti Polar Lipids, Alabaster, AL) and PIPs (Cell Signaling Technology, Beverly, MA) in chloroform were diluted with

spotting buffer (1:1 chloroform:methanol with 0.2% Ponceau S stain) to yield 100–500 pmol/ml. One milliliter of lipids or PIPs was spotted onto Whatman BAS-85 nitrocellulose membranes and dried for 1 h at room temperature in the dark. After incubating the membranes with 1–10 μg/ml of purified protein in Tris-buffered saline and 0.1% Triton X-100 with 0.2% fatty acid–free bovine serum albumin overnight at 4°C, membranes were washed and subsequently processed using standard immunoblotting procedures.

Transferrin preparation and trafficking experiments

For use in BTRD cell experiments, bovine holo transferrin was conjugated to FITC as described (McGraw and Subtil, 1999). Alexa 488–labeled human Tf (Molecular Probes, Invitrogen) was used for HeLa cell experiments. For Tf uptake experiments, HeLa cells or BTRD cells were grown on coverslips for a minimum of 2 d, washed 15 min three times in 37°C MEM or DMEM without serum, and incubated for the indicated pulse time points with 40 μg/ml fluorescent holo Tf in 37°C MEM or DMEM. Cells were then washed three times in 37°C MEM + 10% bovine growth serum or Nu-Serum, with subsequent incubation for chase time points.

Microscopy

Wide-field epifluorescence imaging was done using a Zeiss Axioscope II, with Zeiss 40x or 100x Plan-Apochromat numerical aperture–1.4 objective lenses, a Hamamatsu Orca II digital camera, and Openlab software (Improvision, PerkinElmer, Waltham, MA). Spinning disk confocal images were taken with a Nikon Eclipse TE2000-U, Nikon Plan-Apo 60xA/N1.4, or Nikon Plan-Apo100x/N1.4 oil objective, with PerkinElmer UltraVIEW LCI, a Hamamatsu 1394 ORCA-ER camera, and PerkinElmer UltraVIEW software.

Image analysis and statistics

For Tf trafficking analysis, Tf fluorescence was measured from 40× Zeiss wide-field images using ImageJ to measure total cell fluorescence intensity, central (ERC) fluorescence intensity, and background fluorescence. For each image, the background fluorescence intensity (per pixel) was subtracted from the corresponding cell fluorescence measurements. Total Tf fluorescence corresponds to the total cell fluorescence, percentage of maximum Tf fluorescence corresponds to the total cell fluorescence at the indicated time point as a percentage of total cell fluorescence after 45 min of Tf pulse, and the center Tf fluorescence corresponds to the fluorescence of clustered juxtanuclear Tf fluorescence signal. ERC markers could not be used, as the markers were not compatible with other fluorescence and immunolabeling used.

For determining the percentage of cells with a particular distribution of early and late endosomes, cells with endosomes present or absent in the juxtanuclear region of the cell were qualitatively counted "blind" (i.e., not knowing the experimental condition). Similar qualitative analysis was conducted for determining percentage of cells with central TfR or Tf, where cells were counted for having or lacking a distinct central, juxtanuclear fluorescence spot.

To determine the percentage of endosomes with tubules, Alexa 488–Tf-labeled endosomes (100–370/cell) were counted from two confocal slices 0.4 μm apart, starting 0.8 μm from the cell surface adjacent to the coverslip. Endosomes were counted as spherical (no tubules), with one tubule or with multiple tubules. Tubules were defined as elongated protrusions.

Error bars on graphs represent SE of the mean values for a minimum of 100 cells and a minimum of three independent experiments, unless otherwise specified. Two-tailed, unequal variance Student's *t* tests or analyses of variance (ANOVAs) were used to determine significance.

ACKNOWLEDGMENTS

We thank Z. Derewenda for plasmids encoding PAFAH Ib α1 and α2 and Marci Scidmore (Cornell University College of Veterinary Medicine, Ithaca, NY) and Craig Roy (Yale University School of Medicine, New Haven, CT) for the Rab constructs. We also thank Amy Antosh for technical help with some of the Tf uptake experiments. This work was supported by National Institutes of Health Grant DK51596 to W.J.B.

REFERENCES

Arai H (2002). Platelet-activating factor acetylhydrolase. Prostaglandins Other Lipid Mediat 68–69, 83–94.

Bechler ME, Doody AM, Racoosin E, Lin L, Lee KH, Brown WJ (2010). The phospholipase complex PAFAH Ib regulates the functional organization of the Golgi complex. J Cell Biol 190, 45–53.

Ben-Tekaya H, Kahn RA, Hauri HP (2010). ADP ribosylation factors 1 and 4 and group VIA phospholipase A2 regulate morphology and intraorganellar traffic in the endoplasmic reticulum-Golgi intermediate compartment. Mol Biol Cell 21, 4130–4140.

Bonifacino JS, Glick BS (2004). The mechanisms of vesicle budding and fusion. Cell 116, 153–166.

Bonifacino JS, Rojas R (2006). Retrograde transport from endosomes to the trans-Golgi network. Nat Rev Mol Cell Biol 7, 568–579.

Brown W, Chambers K, Doody A (2003). Phospholipase A2 (PLA2) enzymes in membrane trafficking: mediators of membrane shape and function. Traffic 4, 214–221.

Burd CG, Emr SD (1998). Phosphatidylinositol(3)-phosphate signaling mediated by specific binding to RING FYVE domains. Mol Cell 2, 157–162.

Burkhardt JK, Echeverri CJ, Nilsson T, Vallee RB (1997). Overexpression of the dynamitin (p50) subunit of the dynactin complex disrupts dynein-dependent maintenance of membrane organelle distribution. J Cell Biol 139, 469–484.

Cullen PJ (2008). Endosomal sorting and signalling: an emerging role for sorting nexins. Nat Rev Mol Cell Biol 9, 574–582.

de Figueiredo P, Doody A, Polizotto R, Drecktrah D, Wood S, Banta M, Strang M, Brown W (2001). Inhibition of transferrin recycling and endosome tubulation by phospholipase A2 antagonists. J Biol Chem 276, 47361–47370.

de Figueiredo P, Drecktrah D, Katzenellenbogen J, Strang M, Brown W (1998). Evidence that phospholipase A2 activity is required for Golgi complex and trans Golgi network membrane tubulation. Proc Natl Acad Sci USA 95, 8642–8647.

de Figueiredo P, Drecktrah D, Polizotto R, Cole N, Lippincott-Schwartz J, Brown W (2000). Phospholipase A2 antagonists inhibit constitutive retrograde membrane traffic to the endoplasmic reticulum. Traffic 1, 504–511.

de Figueiredo P, Polizotto R, Drecktrah D, Brown W (1999). Membrane tubule-mediated reassembly and maintenance of the Golgi complex is disrupted by phospholipase A2 antagonists. Mol Biol Cell 10, 1763–1782.

Ding C, Liang X, Ma L, Yuan X, Zhu X (2009). Opposing effects of Ndel1 and 1 or 2 on cytoplasmic dynein through competitive binding to Lis1. J Cell Sci 122, 2820–2827.

Driskell OJ, Mironov A, Allan VJ, Woodman PG (2007). Dynein is required for receptor sorting and the morphogenesis of early endosomes. Nat Cell Biol 9, 113–120.

Geuze H, Slot J, Schwartz A (1987). Membranes of sorting organelles display lateral heterogeneity in receptor distribution. J Cell Biol 104, 1715–1723.

Geuze H, Slot J, Strous G, Lodish H, Schwartz A (1983a). Intracellular site of asialoglycoprotein receptor-ligand uncoupling: double-label immunoelectron microscopy during receptor-mediated endocytosis. Cell 32, 277–287.

Geuze H, Slot J, Strous G, Schwartz A (1983b). The pathway of the asialoglycoprotein-ligand during receptor-mediated endocytosis: a morphological study with colloidal gold/ligand in the human hepatoma cell line, Hep G2. Eur J Cell Biol 32, 38–44.

Hao M, Maxfield F (2000). Characterization of rapid membrane internalization and recycling. J Biol Chem 275, 15279–15286.

Harada A, Takei Y, Kanai Y, Tanaka Y, Nonaka S, Hirokawa N (1998). Golgi vesiculation and lysosome dispersion in cells lacking cytoplasmic dynein. J Cell Biol 141, 51–59.

Hattori M, Adachi H, Tsujimoto M, Arai H, Inoue K (1994). The catalytic subunit of bovine brain platelet-activating factor acetylhydrolase is a novel type of serine esterase. J Biol Chem 269, 23150–23155.

Hattori M, Arai H, Inoue K (1993). Purification and characterization of bovine brain platelet-activating factor acetylhydrolase. J Biol Chem 268, 18748–18753.
He W, Ladinsky MS, Huey-Tubman KE, Jensen GJ, McIntosh JR, Bjorkman PJ (2008). FcRn-mediated antibody transport across epithelial cells revealed by electron tomography. Nature 455, 542–546.
Heller L, Park J, Brown W (1994). Biosynthesis and intracellular transport of a membrane glycoprotein (plgp57) of the prelysosome compartment. Mol Membr Biol 11, 127–134.
Ho YS *et al.* (1997). Brain acetylhydrolase that inactivates platelet-activating factor is a G-protein-like trimer. Nature 385, 89–93.
Kardon JR, Vale RD (2009). Regulators of the cytoplasmic dynein motor. Nat Rev Mol Cell Biol 10, 854–865.
Kato M, Dobyns W (2003). Lissencephaly and the molecular basis of neuronal migration. Hum Mol Genet 12, supp 1, R89–R96.
Kerjan G, Gleeson JG (2007). Genetic mechanisms underlying abnormal neuronal migration in classical lissencephaly. Trends Genet 23, 623–630.
Koizumi H, Yamaguchi N, Hattori M, Ishikawa T, Aoki J, Taketo M, Inoue K, Arai H (2003). Targeted disruption of intracellular type I platelet activating factor-acetylhydrolase catalytic subunits causes severe impairment in spermatogenesis. J Biol Chem 278, 12489–12494.
Lam C, Vergnolle MAS, Thorpe L, Woodman PG, Allan VJ (2010). Functional interplay between LIS1, NDE1 and NDEL1 in dynein-dependent organelle positioning. J Cell Sci 123, 202–212.
Lemmon MA (2008). Membrane recognition by phospholipid-binding domains. Nat Rev Cell Mol Biol 9, 99–111.
Liang Y, Yu W, Li Y, Yang Z, Yan X, Huang Q, Zhu X (2004). Nudel functions in membrane traffic mainly through association with Lis1 and cytoplasmic dynein. J Cell Biol 164, 557–566.
Lippincott-Schwartz J, Yuan L, Tipper C, Amherdt M, Orci L, Klausner RD (1991). Brefeldin A's effects on endosomes, lysosomes, and the TGN suggest a general mechanism for regulating organelle structure and membrane traffic. Cell 67, 601–616.
Manya H, Aoki J, Kato H, Ishii J, Hino S, Arai H, Inoue K (1999). Biochemical characterization of various catalytic complexes of the brain platelet-activating factor acetylhydrolase. J Biol Chem 274, 31827–31832.
Marsh M, Griffiths G, Dean GE, Mellman I, Helenius A (1986). Three-dimensional structure of endosomes in BHK-21 cells. Proc Natl Acad Sci USA 83, 2899–2903.
Maxfield FR, McGraw TE (2004). Endocytic recycling. Nat Rev Mol Cell Biol 5, 121–132.
McGraw TE, Subtil A (1999). Endocytosis: biochemical assays. In: Current Protocols in Cell Biology, Vol. 1, ed. JS Bonifacino, M Dasso, JB Harford, J Lippincott-Schwartz, KM Yamada, New York: John Wiley & Sons, 15.13.11–15.13.23.
Miaczynska M, Zerial M (2002). Mosaic organization of the endocytic pathway. Exp Cell Res 272, 8–14.
Park J, Lopez J, Cluett E, Brown W (1991). Identification of a membrane glycoprotein found primarily in the prelysosomal endosome compartment. J Cell Biol 112, 245–255.
Polizotto RS, de Figueiredo P, Brown WJ (1999). Stimulation of Golgi membrane tubulation and retrograde trafficking to the ER by phospholipase A(2) activating protein (PLAP) peptide. J Cell Biochem 74, 670–683.
Regan-Klapisz E, Krouwer V, Langelaar-Makkinje M, Nallan L, Gelb M, Gerritsen H, Verkleij AJ, Post JA (2009). Golgi-associated cPLA2alpha regulates endothelial cell-cell junction integrity by controlling the trafficking of transmembrane junction proteins. Mol Biol Cell 20, 4225–4234.
Rojas R *et al.* (2008). Regulation of retromer recruitment to endosomes by sequential action of Rab5 and Rab7. J Cell Biol 183, 513–526.
Rome L (1985). Curling receptors. Trends Biochem Sci 10, 151.
San Pietro E *et al.* (2009). Group IV phospholipase A(2)alpha controls the formation of inter-cisternal continuities involved in intra-Golgi transport. PLoS Biol 7, e1000194.
Sato TK, Overduin M, Emr SD (2001). Location, location, location: membrane targeting directed by PX domains. Science 294, 1881–1885.
Sheetz M, Singer S (1974). Biological membranes as bilayer couples. A molecular mechanism of drug-erythrocyte interactions. Proc Natl Acad Sci USA 71, 4457–4461.
Sheff D, Daro E, Hull M, Mellman I (1999). The receptor recycling pathway contains two distinct populations of early endosomes with different sorting functions. J Cell Biol 145, 123–139.
Smith DS, Niethammer M, Ayala R, Zhou Y, Gambello MJ, Wynshaw-Boris A, Tsai LH (2000). Regulation of cytoplasmic dynein behaviour and microtubule organization by mammalian Lis1. Nat Cell Biol 2, 767–775.
Stenmark H, Aasland R, Toh BH, D'Arrigo A (1996). Endosomal localization of the autoantigen EEA1 is mediated by a zinc-binding FYVE finger. J Biol Chem 271, 24048–24054.
Stoorvogel W, Geuze HJ, Strous GJ (1987). Sorting of endocytosed transferrin and asialoglycoprotein occurs immediately after internalization in HepG2 cells. J Cell Biol 104, 1261–1268.
Tarricone C, Perrina F, Monzani S, Massimiliano L, Kim MH, Derewenda ZS, Knapp S, Tsai LH, Musacchio A (2004). Coupling PAF signaling to dynein regulation; structure of LIS1 in complex with PAF-acetylhydrolase. Neuron 44, 809–821.
Traer CJ *et al.* (2007). SNX4 coordinates endosomal sorting of TfnR with dynein-mediated transport into the endocytic recycling compartment. Nat Cell Biol 9, 1370–1380.
Valetti C, Wetzel DM, Schrader M, Hasbani MJ, Gill SR, Kreis TE, Schroer TA (1999). Role of dynactin in endocytic traffic: effects of dynamitin overexpression and colocalization with CLIP-170. Mol Biol Cell 10, 4107–4120.
Vallee RB, Tsai JW (2006). The cellular roles of the lissencephaly gene LIS1, and what they tell us about brain development. Genes Dev 20, 1384–1393.
Wood SA, Brown WJ (1992). The morphology but not the function of endosomes and lysosomes is altered by brefeldin A. J Cell Biol 119, 273–285.
Wood SA, Park JE, Brown WJ (1991). Brefeldin A causes a microtubule-mediated fusion of the trans-Golgi network and early endosomes. Cell 67, 591–600.
Yamada M *et al.* (2008). LIS1 and NDEL1 coordinate the plus-end-directed transport of cytoplasmic dynein. EMBO J 27, 2471–2483.
Yamaguchi N, Koizumi H, Aoki J, Natori Y, Nishikawa K, Natori Y, Takanezawa Y, Arai H (2007). Type I platelet-activating factor acetylhydrolase catalytic subunits over-expression induces pleiomorphic nuclei and centrosome amplification. Genes Cells 12, 1153–1161.
Yan W, Assadi AH, Wynshaw-Boris A, Eichele G, Matzuk MM, Clark GD (2003). Previously uncharacterized roles of platelet-activating factor acetylhydrolase 1b complex in mouse spermatogenesis. Proc Natl Acad Sci USA 100, 7189–7194.
Zimmerberg J, Kozlov MM (2006). How proteins produce cellular membrane curvature. Nat Rev Mol Cell Biol 7, 9–19.